

On the Ruin of Age of Information in Augmented Reality over Wireless Terahertz (THz) Networks

Christina Chaccour and Walid Saad

Wireless@VT, Bradley Department of Electrical and Computer Engineering, Virginia Tech, Blacksburg, VA USA,
Emails:{christinac, walids}@vt.edu.

Abstract—Guaranteeing fresh and reliable information for augmented reality (AR) services is a key challenge to enable a real-time experience and sustain a high quality of physical experience (QoPE) for the users. In this paper, a terahertz (THz) cellular network is used to exchange rate-hungry AR content. For this network, guaranteeing an instantaneous low peak age of information (PAoI) is necessary to overcome the uncertainty stemming from the THz channel. In particular, a novel economic concept, namely, the risk of ruin is proposed to examine the probability of occurrence of rare, but extremely high PAoI that can jeopardize the operation of the AR service. To assess the severity of these hazards, the cumulative distribution function (CDF) of the PAoI is derived for two different scheduling policies. This CDF is then used to find the probability of maximum severity of ruin PAoI. Furthermore, to provide long term insights about the AR content’s age, the average PAoI of the overall system is also derived. Simulation results show that an increase in the number of users will positively impact the PAoI in both the expected and worst-case scenarios. Meanwhile, an increase in the bandwidth reduces the average PAoI but leads to a decline in the severity of ruin performance. The results also show that a system with preemptive last come first served (LCFS) queues of limited size buffers have a better ruin performance (12% increase in the probability of guaranteeing a less severe PAoI while increasing the number of users), whereas first come first served (FCFS) queues of limited buffers lead to a better average PAoI performance (45% lower PAoI as we increase the bandwidth).

Index Terms— Augmented Reality (AR), Age of Information (AoI), Terahertz, Ruin

I. INTRODUCTION

The emergence of wireless eXtended reality (XR) will yield a radical paradigm shift from conventional network designs aiming to fulfill a quality-of-service (QoS), towards ones targeting a new concept dubbed *quality of physical experience (QoPE)* [1]. To maintain a high QoPE, the wireless network should be capable of soliciting its users’ five senses. XR encompasses augmented reality (AR), virtual reality (VR), and mixed reality (MR) as shown in Fig. 1, whose applications will offer a wide range of experiences with different goals. On the virtual end of the spectrum, VR’s main goal is to fully immerse the user in a virtual experience, whereas AR aims to supplement reality with virtual objects. Henceforth, to ensure *immersion*, XR services necessitate visual and haptic requirements that are translated onto a wireless downlink at high-rate and high-reliability low latency communications (HRLLC) as investigated in [2]. Clearly, to exchange XR content at high rate on the downlink and uplink, it is natural

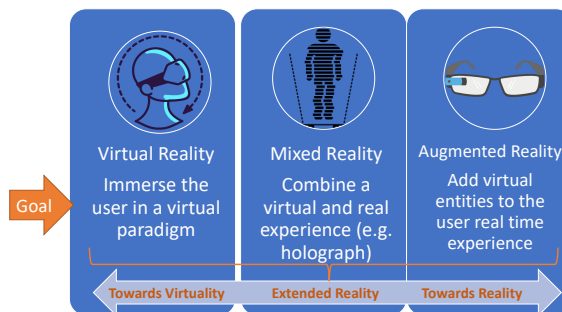


Fig. 1: Illustrative example of the XR spectrum

to adopt frequency bands beyond millimeter wave (mmWave), making the communication at terahertz (THz) band necessary.

Nevertheless, an HRLLC downlink in AR would be serving outdated requests if it is not supplemented with a call for *fresh* information at the uplink. The freshness of this uplink information determines the timeliness of AR requests to the server that generates the AR experiences. Since AR will be used in critical applications (e.g. Google Glass is expected to be heavily deployed by numerous industries ranging from manufacturing all the way to surgical operations [3]) a single disruption caused by an *extreme event*, such as highly outdated/delayed uplink data or an unusual traffic pattern, can lead to substantial hazards. For instance, an obsolete AR request in a biological lab translates into a biohazard that poses threats to the lives of individuals or the security of property. Thus, apart from disrupting the user’s QoPE, outdated information in an AR network will lead to tremendous faults and great risks. To address this challenge, the freshness of information can be quantified by the concept of age of information (AoI). For wireless AR users, AoI depends on both the generation and transmission of AR content while capturing the receiver information freshness. Moreover, given that THz frequencies are necessary to transmit rate-hungry AR content, it is imperative to understand whether an AR wireless network over THz can sustain an instantaneous low AoI to provide the user the promised QoPE.

A. Prior Works

The concept of AoI has recently seen a surge in literature such as in [4]–[6]. In [4], the optimal control of information updates from a source node to a destination was studied. The work in [5] studied the problem of minimizing non-uniform status packet sizes for IoT monitoring systems. The authors in [6] examined the AoI timeliness metric through a variety of queuing systems. Meanwhile, the concept of peak age of information (PAoI) has been studied in [7]–[9]. In [7],

This research was supported by the Office of Naval Research (ONR) under MURI Grant Grant N00014-19-1-2621 and by the National Science Foundation under Grant CNS-1836802.

the authors characterized the average age and the PAoI for different scheduling policies. The authors in [8] investigated the expected PAoI expressions under different scheduling policies. The work in [9] studies the tradeoff between frequency of status updates and queuing delay. However, these works [4]–[9] do not examine the behavior of AoI in providing fresh information to critical and stringent XR applications. In fact, the works in [4]–[9] do not examine the *instantaneous* aging process necessary to deliver a real-time AR experience, thus, they do not shed light on extreme events with a high AoI. Such events lead to substantial risks in critical AR applications and require a study of *the risk of ruin*, i.e., the likelihood of hazardous damages caused by exceeding the PAoI measure. Such an analysis is fundamentally important for a better understanding of the uncertain THz channel.

The main contribution of this paper is a ruin-aware novel performance analysis in terms of achievable average peak AoI, worst-case AoI, and reliability for a cellular network operating at THz frequencies and servicing AR users. The ultimate goal is to assess how and when a THz network can deliver minimal peak AoI, in terms of the THz data rate, depending on the adopted network queuing policies. In particular, we introduce a model for a wireless AR service that is deployed using THz operated reconfigurable intelligent surfaces (RISs). In the studied model, each AR user sends a request to an RIS with mobile edge computing (MEC) capabilities, to solicit new AR content. Given the stringent QoPE requirements of AR services and the uncertainty of the THz channel, it is fundamental to examine the expected and the “ruin” PAoI, which captures the worst-case information obsolescence. Subsequently, to guarantee that the PAoI does not violate the QoPE we derive the cumulative distribution function (CDF) of the maximum severity of ruin, i.e., the distribution characterizing the severity of PAoI exceedances. Moreover, we derive the average PAoI to provide long term insights about the AR response. To our best knowledge, *this is the first work that analyzes the ruin oriented PAoI achieved by AR services over a THz cellular network*. Simulation results show that an increase in the number of users positively impacts the PAoI both in the expected and worst-case, while an increase in the bandwidth reduces the average PAoI but leads to a decline in the severity of ruin performance.

The rest of this paper is organized as follows. The system model and problem formulation are presented in Section II. The ruin-oriented peak AoI analysis is performed in Section III. Section IV presents the simulation results. Finally conclusions are drawn in Section V.

II. SYSTEM MODEL AND PROBLEM FORMULATION

Consider the uplink¹ of an RIS-based wireless network in a confined indoor area, servicing a set \mathcal{U} of U mobile wireless AR users via a set \mathcal{B} of B RISs acting as THz operated base stations (BSs). In particular, RISs are a scaled-up

¹The downlink of AR transmission is assumed to follow an arbitrary THz scheme and is outside of the scope of this chapter

version of massive multiple-input and multiple-output (MIMO) that supplement existing walls and structures with wireless capabilities. Thus, RISs increase the likelihood of a near-field communications through a line-of-sight (LoS) path that is fundamental for reliable THz communications². Moreover, the AR users are mobile and may change their locations and orientations at any point in time. We consider continuous time slots indexed by t with fixed duration τ . Each RIS is a BS, that is provided with a feeder (antenna) with a corresponding transmit power denoted by p . Hence, the transmitted data is encoded onto the phases of the signals reflected from different reconfigurable meta-surfaces that compose the RIS [11]. Henceforth, if the RIS consists of N meta-surfaces whose reflection phase can be optimized independently, then an N -stream virtual MIMO system can be realized by using a single radio frequency (RF) active chain [11]. We assume that the RF source is close enough to the RIS surface so that the transmission between each pair of RF source and RIS is not affected by fading [11].

A. Wireless Capacity

We consider an arbitrary AR user u in \mathcal{U} that is at a constant distance d_{ub} from its respective RIS b . Moreover, as a byproduct of directional beamforming, propagation differences, and RIS deployment, the considered network will be noise limited. Furthermore, deploying RISs enables the desired channel to become a LoS channel [12]. Subsequently, to guarantee a LoS link for every AR user, we assume that the RIS-AR user association is performed by a centralized controller [13]. In particular, the electromagnetic response of the N meta-surface elements is programmed by generating input signals that tune varactors and change the phase of the reflected signal [14]. Let $\Theta_{ub,t} = [\theta_{ubn,t}]_{N \times 1}$ be the phase shift vector of RIS b , with respect to user equipment (UE) u , at time slot t , where $\theta_{ubn,t} \in \Theta$, n is the index corresponding to the meta-surface of each RIS, and $\Theta = \{-\pi + \frac{2k\pi}{K-1} | k = 0, 1, \dots, K-1\}$. K is the number of possible phase shifts per meta-surface element. Thus, the random channel gain between AR UE u at time slot t is given by [2]: $h_{ub,t} = \left(\frac{\lambda}{4\pi d_{ub,t}}\right)^2 (e^{-k(f)d_{ub,t}})^2$, where $k(f)$ is the overall molecular absorption coefficient of the medium at the THz band, and f is the operating frequency. Let $\psi_{ubn,t}$ be the phase shift vector between AR UE u and the metasurface n of RIS b at time t . Since the coherence bandwidth at THz is inherently large due to the delay spread and temporal broadening effects as shown in [15] and [16], we can assume that the rate shows an invariant behavior across the THz bandwidth for all the distances considered. Hence, for a given reflection phase shift vector, $\theta_{ub,t}$, the transmission rate from AR UE u to RIS b will be (under an approximate average signal-to-interference-plus-noise-ratio (SINR) value across the THz band):

²The analysis of the probability of blockage is outside the scope of this work, a guaranteed LoS link is assumed since we use RISs [11] deployed on existing walls and structures at a close proximity of the users.

$$R_{ub,t} = W \log_2 \left(1 + \frac{p h_{ub,t} |\sum_{n=1}^N e^{(\theta_{ubn,t} - \psi_{ubn,t})j}|^2}{N(d_{ub,t}, p, f)} \right),$$

where $N(d_{ub,t}, p, f) = N_0 + \sum_{b=1}^B p A_0 d_{ub,t}^{-2} (1 - e^{-K(f)d_{ub,t}})$, $N_0 = \frac{W \lambda^2}{4\pi} k_B T_0$, k_B is the Boltzmann constant, T_0 is the temperature in Kelvin, $A_0 = \frac{c^2}{16\pi^2 f^2}$, and c is the speed of light [2], [17]. Note that the optimal choice for $\theta_{ubn,t}$ for every RIS association is equal to $\psi_{ubn,t}$, thus maximizing the rate $r_{ub,t}$, as shown in [11].

Furthermore, the rate of AR content transmission over the THz link between AR user u and RIS b , assuming a constant image size M , is given by: $r_{ub,t} = \frac{R_{ub,t}}{M}$.

B. Age of Information

The AoI is a key performance metric to quantify the freshness of the status information update at the receiver defined as the time elapsed since the most recent AR content update delivered at the MEC server. By definition, the AoI at the receiver at the beginning of time slot t is given by: $A_{ub,t} = t - U_t^B$, where U_t^B is the time stamp of the freshest AR content update that was delivered to the RIS before t . Moreover, while the use of average AoI as a freshness metric might guarantee a good performance on the long run, for real-time applications such as AR, it is necessary to examine the *instantaneous* aging of information, so as to, capture real-time disruptions to the AR experience. Subsequently, our interest lies in evaluating the distribution of the PAoI and its worst-case performance. In [18], the authors have shown that the AoI is minimized when the queuing follows a last come first served (LCFS) scheme in contrast to an FCFS scheme, also, an LCFS with preemption performed better than an LCFS scheduling without preemption. Nevertheless, this hypothesis is true for queuing schemes with one source, or when all the transmitters are sending out status updates about the same situation. In other words, the freshest update among all sources is always the most desirable update to the receiver. Also, this analysis was solely based on average AoI values and overlooked the instantaneous performance.

In our model, while one user is immersed into one AR session and needs to convey its freshest information to the MEC server, another AR user might be undergoing the same process. On the one hand, we need to ensure a fair scheduling among users and deliver every request freshly to the server, thus, doing so with an FCFS queue allows this process. On the other hand, in case the user needs to urgently deliver a new request, it would be best for the server to ignore the previous requests coming from that user and respond to the most recent one. For example, in a manufacturing plant, if an AR user commits a fault and needs an urgent AR content assistance in solving the situation, an LCFS queuing policy would be the most appropriate for this situation. Otherwise, not only outdated information will be sent, but *risk-inducing outdated information* will be sent to the AR user. Therefore, to scrutinize this problem, we propose to split the queuing system into two as shown in Fig. 2. Splitting the queuing system

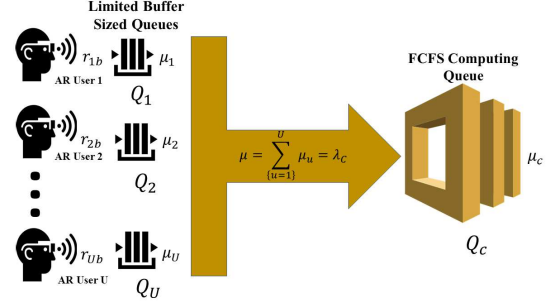


Fig. 2: Illustrative example of our queuing model

allows us to diagnose the complex scheduling situation and to characterize the freshness of the information as a function of fair and priority scheduling policies. Here, similar to [6] and [19], we assume that the AR update arrivals are modeled as a independently and identically distributed (i.i.d.) Poisson point process (PPP) with temporal mean rate $r_{ub} = \mathbb{E}[r_{ub,t}]$. These AR updates are processed and halted in limited sized M/M/1/x queues (x is the buffer size) and then sent to a common FCFS queue, where a new AR content is generated as a response to the status update. Such limited sized queues that provide halting allow us to inject a sense of prioritization to users without leading to an unfair scheduling policy as in with a complete LCFS queue, i.e., priority only when necessary.

According to Burke's Theorem [20], when the service rate is larger than the arrival rate for an M/M/1 queue, then the departure process at steady state is a Poisson process with the same arrival rate. Hence, the arrival of requests to Q_c also follows a Poisson process with rate $\lambda_c = \sum_{u=1}^U \mu_u$, where μ_u is the service rate of each limited buffer sized queue. We also assume that the computing follows a Markovian process and thus, Q_c is an M/M/1 queue with service rate μ_c . Next, we will analyze two types of limited sized queues with different dynamics and buffers. Given the risks pertaining to outdated AR requests, we use a financial concept, the *risk of ruin*, defined as an insurer's likelihood of losing an investment capital [21] and apply it to critical AR requests to characterize the likelihood of hazardous damages based on the aging process. In particular, we derive the ruin of going above a PAoI threshold set for this network and the CDF of maximum severity of ruin. We then compare this ruin-oriented result performance to the average PAoI performance.

III. RUIN-ORIENTED PEAK AOI ANALYSIS

In this section, we examine the instantaneous PAoI and use it to derive the probability of ruin of PAoI. Furthermore, we evaluate the average PAoI pertaining to the overall queuing system and compare its performance to the worst-case PAoI, hence shedding light on the complementarity of their insights and necessity of both average and tail analyses.

A. Instantaneous and Ruin AoI

Here, we analyze the performance of the peak AoI of AR generated content at THz frequency with respect to a limited size FCFS M/M/1/2 queue and an LCFS M/M/1/2* queue, which allows preemption only in waiting, i.e., once an AR content is sent to the computing queue it cannot be preempted. These two types will be evaluated based on the ruin of peak

AoI and its maximum severity.

Hereinafter, the term *reliability* is defined as the ability of the THz network to maintain low PAoI. Moreover, analyzing the reliability of the network in terms of PAoI needs to be performed *instantaneously* and needs to account for the extreme events that will violate the QoPE target performance. In the light of this, we propose a novel notion of ruin-based reliability analysis developed using notions from the powerful actuarial sciences and economics framework [21]–[23]. From economics, the probability of ruin in finite time is defined as:

$$\Psi(u, t) = \Pr(U(s) < 0 \quad \text{for some } s, 0 < s \leq t),$$

where $U(s) = u + ct - S(s)$, u is the insurer's surplus at time 0 and c is the insurer's rate of premium income per unit time, which we assume to be received continuously. Thus, $\Psi(u, t)$ is the probability that the insurer's surplus falls below zero at some time in the future, i.e., the claims outgo exceeds the initial surplus plus premium income. This is a probability of ruin in continuous time, we can similarly define a discrete time ultimate ruin probability. Moreover, the insurer's surplus in the financial domain, translates onto reliability in a wireless network. Moreover, a duality exists between the queuing dynamics of an M/G/1 queue and the risk of ruin as shown in [22]. Elaborating on this duality, we can define the system reliability in terms of PAoI and let $\Psi(u, t)$ characterize its CDF. Subsequently, we will find this distribution and use it to derive the maximum severity of ruin for each one of the scheduling schemes considered.

We first evaluate the probability distribution function (PDF) of the peak AoI for both scheduling configurations. To do so, we define $P(\nu) = \frac{\mu_u}{r_{ub} + \mu_u}$ as the steady state probability as the system is empty, this probability is used to compute the peak AoI PDF, whose conditional is given by: $\Phi(a|\nu) = \Phi(\tau|\nu) * \Phi(y|\nu)$, where a denotes the value of peak AoI, τ is the time spent in the system, and y is the interdeparture time. Thus, knowing the conditional PDFs from [7], we can write the marginal PDF by using Bayes' theorem as follows:

$$\begin{aligned} \Phi_F(a) &= \Phi_F(a|\nu)P(\nu) + \Phi_F(a|\bar{\nu})P(\bar{\nu}), \\ &= \left(\frac{\mu_u}{r_{ub} - \mu_u}\right)^2 r_{ub} (e^{-r_{ub}a} - e^{-\mu_u a} + (r_{ub} - \mu_u) \times \\ &\quad a e^{-\mu_u a}) \left(\frac{\mu_u}{r_{ub} + \mu_u}\right) + \frac{1}{2} a^2 \mu_u^3 e^{-\mu_u a} \left(\frac{r_{ub}}{r_{ub} + \mu_u}\right). \end{aligned} \quad (1)$$

Following a similar procedure for the M/M/1/2* queue, the peak AoI PDF of each queue is given by:

$$\begin{aligned} \Phi_L(a) &= \Phi_L(a|\nu)P(\nu) + \Phi_L(a|\bar{\nu})P(\bar{\nu}), \\ &= \left(\left(r_{ub}(r_{ub} + \mu_u)a - \frac{(2\mu_u^3 - r_{ub}^3 - r_{ub}^2\mu_u)}{\mu_u(r_{ub} - \mu_u)} \right) e^{-(r_{ub} + \mu_u)a} \right. \\ &\quad \left. + \frac{r_{ub}\mu_u + 2\mu_u^2}{r_{ub} - \mu_u + u} e^{-\mu_u a} - \frac{r_{ub}\mu_u(r_{ub} + \mu) + r_{ub}^3}{\mu_u(r_{ub} - \mu_u)} e^{-r_{ub}a} \right) \\ &\quad \times \left(\frac{\mu_u}{r_{ub} + \mu_u} \right) + \left(\frac{\mu_u^2}{r_{ub}^2} e^{-(r_{ub} + \mu_u)a} (3\mu_u + 2r_{ub} + r_{ub}(r_{ub} + \mu_u)a) \right. \\ &\quad \left. - \frac{\mu_u^2}{r_{ub}^2} e^{-\mu_u a} (3\mu_u + 2r_{ub} - r_{ub}(r_{ub} + 2\mu_u)a) \right) \times \left(\frac{r_{ub}}{r_{ub} + \mu_u} \right). \end{aligned} \quad (2)$$

Henceforth, to examine the worst-case scenario, i.e., the greatest AoI peak, we consider the *maximum severity of ruin* given the one-to-one relation between any M/G/1 system and a ruin probability.³ Thus, the ruin characterization of system reliability allows us to capture the effect of extreme events on the immersive real-time response. In other words, the maximum severity of ruin characterizes the severity of the worst peak QoPE of the AR user. Next, we derive the CDF of the maximum severity of PAoI ruin.

Theorem 1. *The CDF characterizing the maximum severity of PAoI, for a PAoI threshold of z is given by:*

$$J_F(z) = \Pr(M_F \leq z | a < \infty) = \frac{\Psi_F(a) - \Psi_F(a+z)}{\Psi_F(a)(1 - \Psi_F(z))}, \quad (3)$$

$$J_L(z) = \Pr(M_L \leq z | a < \infty) = \frac{\Psi_L(a) - \Psi_L(a+z)}{\Psi_L(a)(1 - \Psi_L(z))}. \quad (4)$$

where $\Psi_F(a)$ is the CDF of PAoI over M/M/1/2 FCFS queues scheduling policies, $\Psi_L(a)$ is the CDF of PAoI over M/M/1/2* LCFS queues scheduling policies, $M_F = \sup \{A_F(t) | a < \infty\}$, $M_L = \sup \{A_L(t) | a < \infty\}$, $A_F(t)$ is the peak AoI experienced at time t over M/M/1/2 FCFS queues scheduling policies, and $A_L(t)$ is the peak AoI experienced at time t over M/M/1/2* LCFS queues scheduling policies. Thus, M_F and M_L are the worst-case peak AoI for each case.

Proof: See Appendix A ■

This result allows us to tractably assess the conditions during which worst-case PAoIs will not exceed a worst-case threshold z . The CDFs of both scheduling policies is a function of the THz data rate and the queuing service rate. As long as the maximum severity of ruin PAoI is maintained below z , a reliable, real-time response will be provided to the AR user and the QoPE will not be violated in extreme events.

B. Average Peak AoI

In addition to the severity of ruin computed for the limited buffer size queues, we evaluate the average end-to-end (E2E) peak AoI of our system. Given that Q_c is an M/M/1 queue, the average peak AoI can be given by [24]: $\hat{A}_c = \frac{1}{\lambda_C} + \frac{1}{\mu_C} + \frac{\lambda_C(\mu_C + \mu_C^2)}{2(1 - \rho_C)}$, where $\rho_C = \frac{\lambda_C}{\mu_C}$. Subsequently, the average E2E peak AoI can be given for each case as:

$$\begin{aligned} \hat{A}_F &= \frac{1}{\lambda_C} + \frac{1}{\mu_C} + \frac{\lambda_C(\mu_C + \mu_C^2)}{2(1 - \rho_C)} \\ &\quad + \sum_{u=1}^U \left(\frac{1}{r_{ub}} + \frac{3}{\mu_u} - \frac{2}{(r_{ub} + \mu_u)} \right), \end{aligned} \quad (5)$$

$$\begin{aligned} \hat{A}_L &= \frac{1}{\lambda_C} + \frac{1}{\mu_C} + \frac{\lambda_C(\mu_C + \mu_C^2)}{2(1 - \rho_C)} \\ &\quad + \sum_{u=1}^U \left(\frac{1}{r_{ub}} + \frac{1}{\mu_u} + \frac{r_{ub}}{(r_{ub} + \mu_u)^2} + \frac{r_{ub}}{\mu_u(r_{ub} + \mu_u)} \right). \end{aligned} \quad (6)$$

Here, in addition to our worst-case scenario analysis, the average PAoI provides us with long term insights about PAoI

³The aggregation of our limited size queues and FCFS computing queue constitutes an M/G/1 queue.

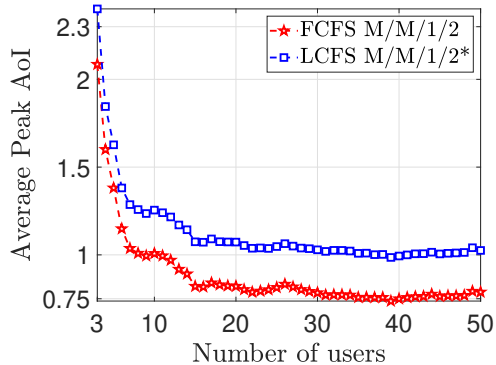


Fig. 3: Average peak AoI versus number of users

pertaining to a fair non extreme scenario. Moreover, here we also consider the computing queue in the aging process to provide us with the E2E aging peak. Next, in our simulation results, we compare the two suggested schemes and contrast the differences in their behavior from an expected and worst-case viewpoint.

IV. SIMULATION RESULTS AND ANALYSIS

For our simulations, we consider the following parameters: $T_0 = 300$ K, $p = 1$ W, $M = 10$ Mbits, $f = 1$ THz, $W = 10$ GHz, $K(f) = 0.0016 \text{ m}^{-1}$ with 1% of water vapor molecules as in [25] and we have chosen $\mu_i = 5$ packets/s $\mu_c = 100$ packets/s these values are chosen to comply with existing AR processing units such as the GEFORCE RTX 2080 Ti [26]. The RISs are deployed over the 4 walls of an indoor area modeled as a square of size $50 \text{ m} \times 50 \text{ m}$.

Fig. 3 and Fig. 4 show the effect of the density of users on the freshness of information. We can see in Fig. 3 that the peak average AoI monotonically decreases with the number of users in the area. This is due to the fact that more packets are arriving simultaneously bringing fresher information into the network's server. In contrast to a typical E2E delay analysis, an increase in the number of users would degrade the E2E delay, while it improves the age as shown here. Moreover, the FCFS M/M/1/2 queue's average PAoI is 35% lower than the LCFS M/M/1/2* queue for all densities. The gap between the two schemes increases as the number of users increases.

Moreover, in Fig. 4, we evaluate the distribution of worst-case peak AoI below a threshold, where the threshold is set to $z = 3$. This threshold was set based on the range of average PAoI to contrast ruin behaviors to the expected one. Here, the number of users also positively impacts the performance, as the probability of the worst-case peak AoI below z , is increasing with the number of users. Thus, as the density of users increases, the worst-case performance is further guaranteed to be below $z = 3$. Nevertheless, even though the LCFS M/M/1/2* queue had a higher average peak AoI, it is shown here that it performs 12% better in terms of worst-case performance, and thus provides fresher information during *extreme and dynamic events* when the number of users increases. In particular, LCFS allow AR users to deliver their more urgent requests while preempting their previous requests.

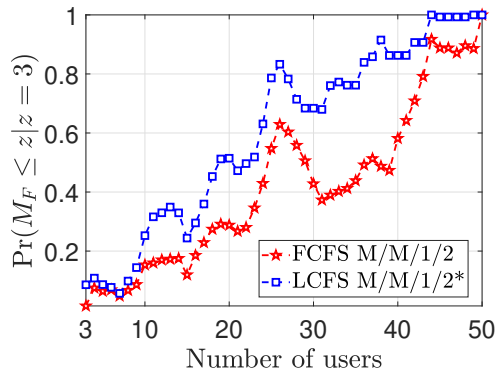


Fig. 4: Probability of worst-case peak AoI below $z = 3$ versus number of users.

This is especially useful during extreme events, that might delay urgent requests given that is incurring more latency to process the previous requests, and leading LCFS M/M/1/2* queue will alleviate this issue.

Fig. 5 and Fig. 6 show the prominent effect of the bandwidth on the freshness of information, for $U = 15$ users. We can see in Fig. 5 that the peak average AoI monotonically decreases with a higher bandwidth, this also corresponds to the fact that a higher number packets is arriving per unit time, thus ensuring information at the network's server. In here, the FCFS M/M/1/2 queue's average peak AoI is 45% lower than the LCFS M/M/1/2* queue for all values of the bandwidth. The gap between the two schemes increases as the bandwidth increases.

Moreover, in Fig.6 we evaluate the distribution of worst-case peak AoI, where the threshold is set to $z = 3$. Here, and in contrast to the scenario of users density, the increase in bandwidth negatively impacts the ruin performance, i.e., the probability of a worst-case peak AoI below z , is decreasing as the bandwidth increases. Clearly, a higher bandwidth changes the frequency range of THz, thus, implying complications in terms of molecular absorption effect and range of operation, finally leading to extreme events with negative impact. Henceforth, increasing the bandwidth will increase the data rate and improve the performance of peak AoI on average but will shift the worst-case peak AoI to higher values. Here also, similarly to the density of the users, the LCFS behaves better in terms of extreme events, but worse in terms of average peak AoI performance.

V. CONCLUSION

In this paper, we have studied the AoI of AR services in a THz cellular network employing RISs as its BSs. We have performed a novel ruin-aware performance analysis that scrutinizes the PAoI during extreme events. After deriving the PAoI CDFs, we have used it to find the CDF of the maximum severity of ruin for different scheduling policies. Moreover, we have also derived the average PAoI for our considered model and compared the ruin performance analysis to the average PAoI and contrasted the differences in the behavior. While introducing LCFS preempting limited sized queues improved the ruin performance, FCFS limited sized queues improved the average PAoI performance.

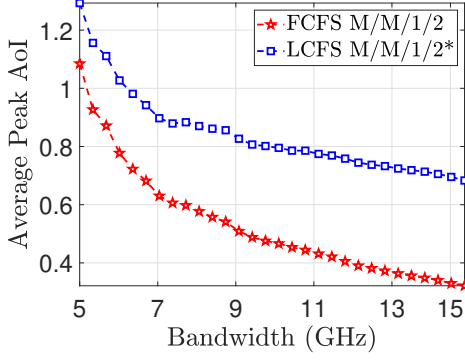


Fig. 5: Average peak AoI versus bandwidth

APPENDIX

A. Proof of Theorem 1

Proof: Given that the maximum severity of ruin is a function of the CDF of ruin, we first need to integrate the results in (1) and (2). After some mathematical manipulations, we obtain the CDFs for the FCFS M/M/1/2 queue and the LCFS M/M/1/2* respectively:

$$\varphi_F(a) = 1 - \frac{\mu_u^3}{(r_{ub} - \mu_u)^2(r_{ub} + \mu_u)} e^{-r_{ub}a} - \frac{r_{ub}}{2(r_{ub} - \mu_u)^2(r_{ub} + \mu_u)} e^{-\mu_u a} \times [\mu_u^2 a^2 (r_{ub} - \mu_u)^2 + 2r_{ub}\mu_u(r_{ub} - \mu_u)a + 2(r_{ub}^2 - r_{ub}\mu_u - \mu_u^2)], \quad (7)$$

$$\varphi_L(a) = 1 - \frac{e^{-(r_{ub} + \mu_u)a}}{r_{ub}(r_{ub} + \mu_u)(r_{ub} - \mu_u)} (r_{ub}^3 - 3\mu_u^3 + r_{ub}\mu_u(r_{ub} + \mu_u)(1 + (r_{ub} - \mu_u))) + \frac{e^{-r_{ub}a}}{(r_{ub} + \mu_u)(r_{ub} - \mu_u)} \times (r_{ub}^2 + r_{ub}\mu_u + \mu_u^2) - \frac{e^{-\mu_u a}}{r_{ub}(r_{ub} + \mu_u)(r_{ub} - \mu_u)} (3\mu_u^3 + r_{ub}(r_{ub} - \mu_u)^2 + r_{ub}\mu_u a (r_{ub}^2 + r_{ub}\mu_u - 2\mu_u^2)). \quad (8)$$

Moreover, given that the AR updates are i.i.d., the CDF of the AoI at the end of all limited buffer sized queues is given by:

$$\Psi_F(a) = (\varphi_F(a))^u, \quad \Psi_L(a) = (\varphi_L(a))^u. \quad (9)$$

Hence, the distribution of the maximum severity of ruin in each case can be given according to its definition in [21] by the result in (3) and (4) in Theorem 1. ■

REFERENCES

- [1] W. Saad, M. Bennis, and M. Chen, "A vision of 6G wireless systems: Applications, trends, technologies, and open research problems," *IEEE Network*, 2020.
- [2] C. Chaccour, M. N. Soorki, W. Saad, M. Bennis, and P. Popovski, "Can terahertz provide high-rate reliable low latency communications for wireless VR?" *arXiv preprint arXiv:2005.00536*, 2020.
- [3] B. John and N. Wickramasinghe, "A review of mixed reality in health care," in *Delivering Superior Health and Wellness Management with IoT and Analytics*. Springer, Nov. 2019, pp. 375–382.
- [4] Y. Sun, E. Uysal-Biyikoglu, R. D. Yates, C. E. Koksak, and N. B. Shroff, "Update or wait: How to keep your data fresh," *IEEE Transactions on Information Theory*, vol. 63, no. 11, pp. 7492–7508, Aug. 2017.
- [5] B. Zhou and W. Saad, "Minimum age of information in the internet of things with non-uniform status packet sizes," *IEEE Transactions on Wireless Communications*, Dec.

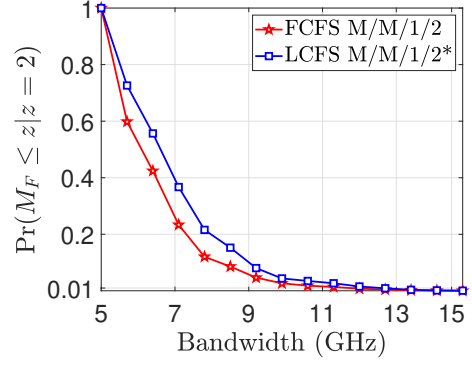


Fig. 6: Probability of worst-Case peak AoI below $z = 2$ versus bandwidth

- [6] R. D. Yates and S. K. Kaul, "The age of information: Real-time status updating by multiple sources," *IEEE Transactions on Information Theory*, vol. 65, no. 3, pp. 1807–1827, Sep. 2018.
- [7] M. Costa, M. Codreanu, and A. Ephremides, "On the age of information in status update systems with packet management," *IEEE Transactions on Information Theory*, vol. 62, no. 4, pp. 1897–1910, Feb. 2016.
- [8] K. Chen and L. Huang, "Age-of-information in the presence of error," in *2016 IEEE International Symposium on Information Theory (ISIT)*, Barcelona, Spain, Jul. 2016, pp. 2579–2583.
- [9] L. Huang and E. Modiano, "Optimizing age-of-information in a multi-class queueing system," in *Proc. of International Symposium on Information Theory (ISIT)*, Hong Kong, China, Jun. 2015, pp. 1681–1685.
- [10] A. Kosta, N. Pappas, A. Ephremides, and V. Angelakis, "Non-linear age of information in a discrete time queue: Stationary distribution and average performance analysis," *arXiv preprint arXiv:2002.08798*, 2020.
- [11] E. Basar, M. Di Renzo, J. De Rosny, M. Debbah, M.-S. Alouini, and R. Zhang, "Wireless communications through reconfigurable intelligent surfaces," *IEEE Access*, vol. 7, pp. 116 753–116 773, 2019.
- [12] M. Jung, W. Saad, Y. Jang, G. Kong, and S. Choi, "Reliability analysis of large intelligent surfaces (liss): Rate distribution and outage probability," *IEEE Wireless Communications Letters*, vol. 8, no. 6, pp. 1662–1666, 2019.
- [13] C. Chaccour, M. N. Soorki, W. Saad, M. Bennis, and P. Popovski, "Risk-based optimization of virtual reality over terahertz reconfigurable intelligent surfaces," in *Proc. of IEEE International Conference on Communications (ICC)*, Dublin, Ireland, June. 2020.
- [14] C. Huang, A. Zappone, G. C. Alexandropoulos, M. Debbah, and C. Yuen, "Reconfigurable intelligent surfaces for energy efficiency in wireless communication," *IEEE Transactions on Wireless Communications*, vol. 18, no. 8, pp. 4157–4170, 2019.
- [15] J. Kokkonieni, J. Lehtomäki, K. Umehayashi, and M. Juntti, "Frequency and time domain channel models for nanonetworks in terahertz band," *IEEE Transactions on Antennas and Propagation*, vol. 63, no. 2, pp. 678–691, Feb. 2015.
- [16] C. Han, W. Tong, and X.-W. Yao, "MA-ADM: A memory-assisted angular-division-multiplexing MAC protocol in terahertz communication networks," *Nano communication networks*, vol. 13, pp. 51–59, Aug. 2017.
- [17] R. Zhang, K. Yang, Q. H. Abbasi, K. A. Qaraqe, and A. Alomainy, "Analytical modelling of the effect of noise on the terahertz in-vivo communication channel for body-centric nano-networks," *Nano communication networks*, vol. 15, pp. 59–68, 2018.
- [18] S. K. Kaul, R. D. Yates, and M. Gruteser, "Status updates through queues," in *Proc. of 46th Annual Conference on Information Sciences and Systems (CISS)*, 2012, pp. 1–6.
- [19] A. Javani, M. Zorghi, and Z. Wang, "Age of information in multiple sensing," *arXiv preprint arXiv:1902.01975*, 2019.
- [20] D. Gross and C. M. Harris, "Fundamentals of queueing theory," *John Wiley and Sons, New York*, 2008.
- [21] D. C. Dickson, *Insurance risk and ruin*. Cambridge University Press, 2016.
- [22] F. Michaud, "Estimating the probability of ruin for variable premiums by simulation," *ASTIN Bulletin: The Journal of the IAA*, vol. 26, no. 1, pp. 93–105, 1996.
- [23] F. Liu and R. Wang, "A theory for measures of tail risk," *Available at SSRN 2841909*, 2016.
- [24] A. Kosta, N. Pappas, V. Angelakis et al., "Age of information: A new concept, metric, and tool," *Foundations and Trends® in Networking*, vol. 12, no. 3, pp. 162–259, 2017.
- [25] C.-C. Wang, X.-W. Yao, C. Han, and W.-L. Wang, "Interference and coverage analysis for terahertz band communication in nanonetworks," in *Proc. IEEE Global Communications Conference (GLOBECOM)*, Singapore, Dec. 2017.
- [26] GEFORCE RTX 2080 Ti. [Online]. Available: <https://www.nvidia.com/en-us/geforce/graphics-cards/rtx-2080-ti/>